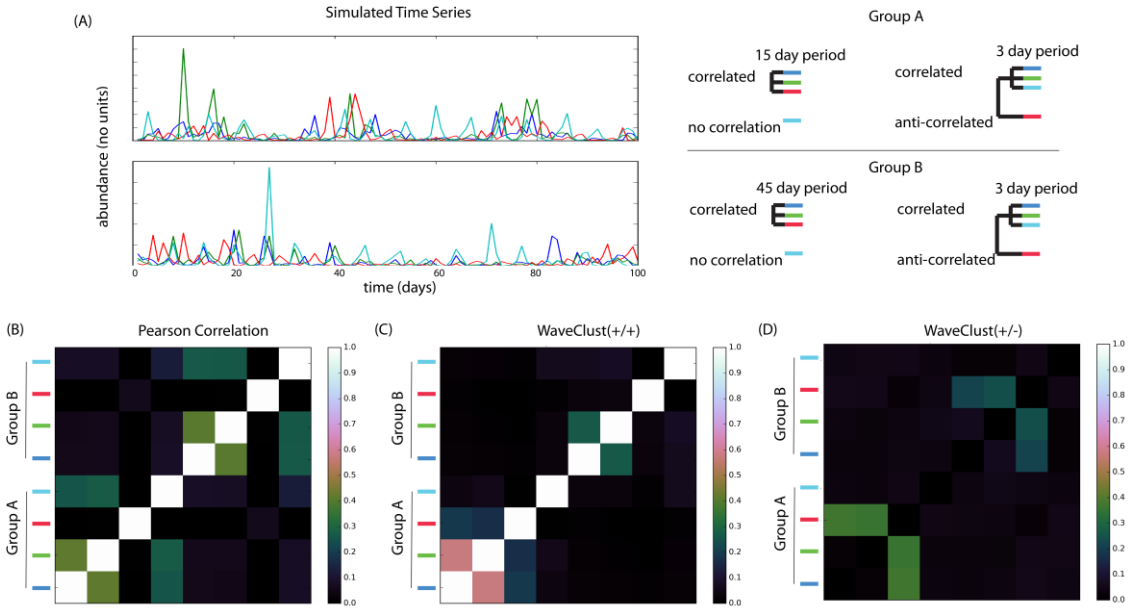

Supplementary Fig. 1 | WaveClust performance with simulated coupled dynamics. We simulated time series with noisy coupled dynamics, consisting of perfect coupling (correlation or anti-correlation) at one or more periods (3 day, 15 day, or 45 day) with the addition of random noise to each series (signal-to-noise ratio: 1). In panel **(A)** the blue and green series are correlated at both high and low frequency (high frequency at 3 day period, low frequency at 15 day period in "Group A" and 45 day period in "Group B"). Both blue and green are correlated with the red series at low frequency, but anti-correlated at high frequency. Thus, the pairs (blue, green) and (blue/green, red) share "emergent" periods at low frequency, but have different high frequency interactions. The teal time series is correlated at high frequency with blue and green, but shares no low frequency correlation. In panel **(B)** we calculate the pairwise Pearson correlation for all series in both Group A and Group B. While this correlation separates the two groups, it has the undesirable effect of grouping the teal series with blue and green, and it finds no relationship between blue or green and red. In panel **(C)**, WaveClust(+/+) is specifically sensitive to the (blue, green) pair, while in **(D)** WaveClust(+/-) is specifically sensitive to (blue/green, red) pairs. Similarity results reflect the average similarity calculated for each pair across 500 random trials.

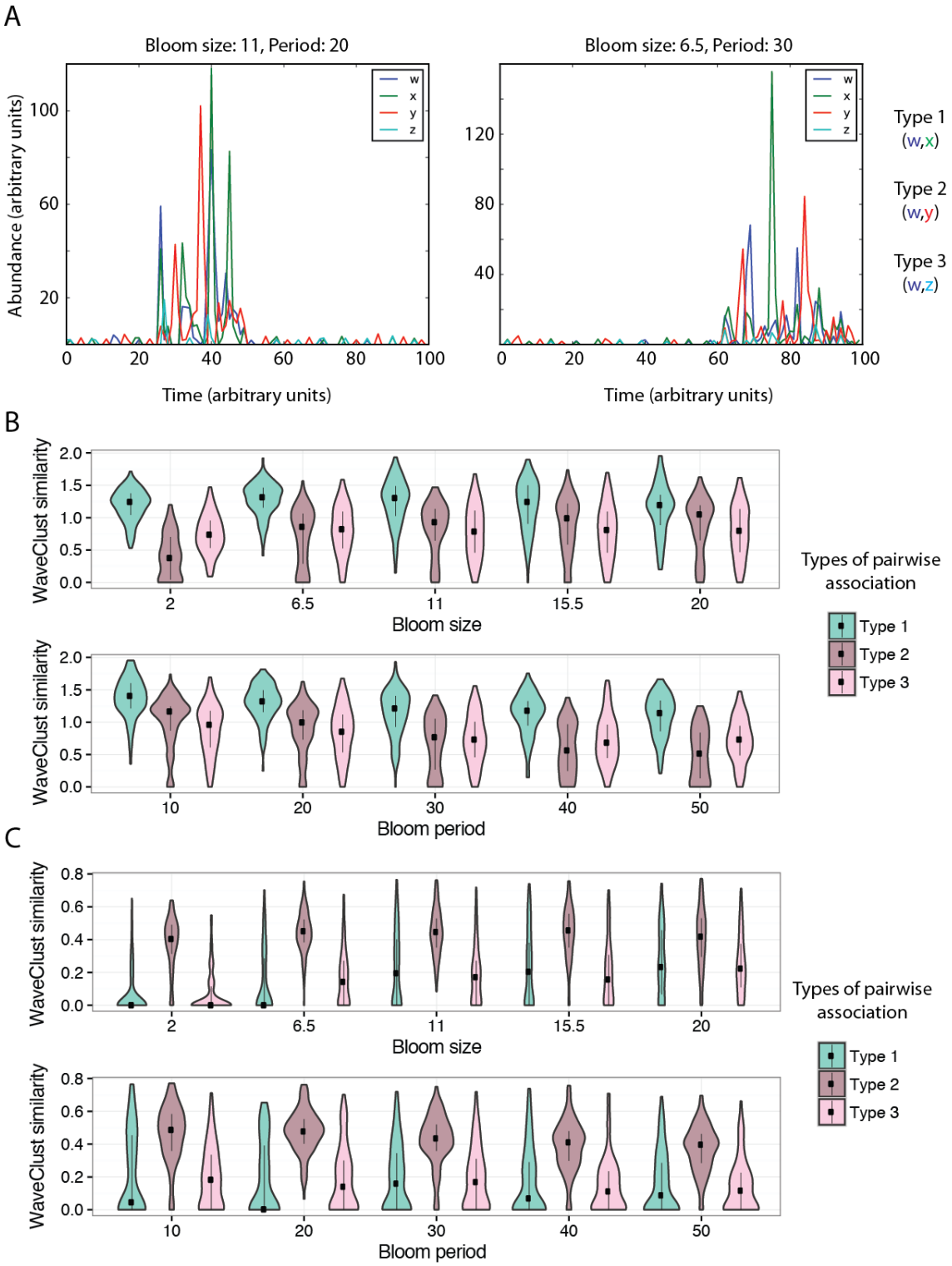

Supplementary Fig. 2 | Sensitivity analysis of WaveClust similarity with simulated data. Time series were simulated to capture patterns of blooms (occurring at low frequency and higher abundance) in the midst of basal fluctuations (occurring at high frequency and lower abundance) with the addition of random noise. Pairs of OTUs with a Type 1 association are correlated at both low and high frequency. Type 2 associations are correlated low frequency, and anti-correlated at high frequency. Type 3 associations are correlated at high frequency, and uncorrelated at low frequency. **(A)** Representative

time series with different bloom size and period (left and right panels). **(B and C)** Violin plots of WaveClust similarity scores (Y axis) between pairs of simulated OTUs with Type 1, 2, or 3 associations, with varying bloom size and period (X axis). Similarity scores are calculated using positive correlation at low frequency, and either positive **(B)** or negative **(C)** correlation at low frequency. Type 1 associations are more easily detected in **(B)**, while Type 2 associations are more easily detected in **(C)**.

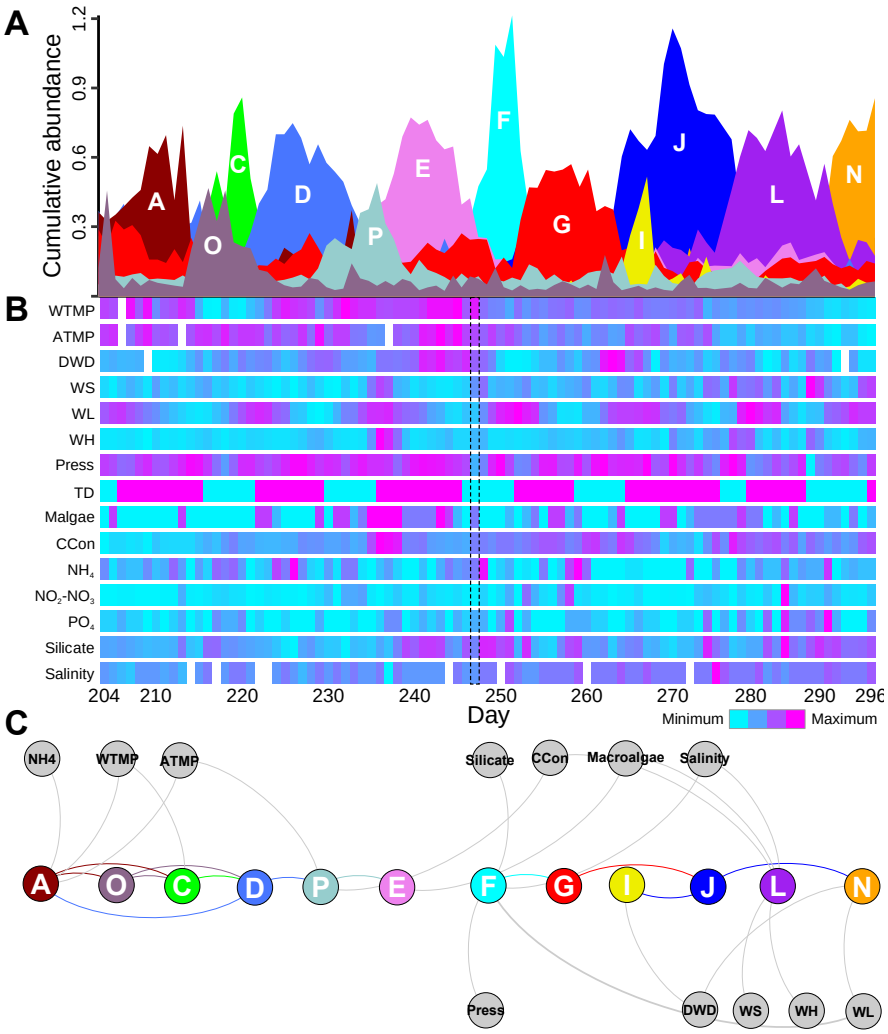

Supplementary Fig. 3 | Dynamics of predicted communities and metadata across the time series. (A) Communities predicted by WaveClust analysis as modular units (clusters) of interacting OTUs based on wavelet decomposition to determine correlations at different temporal frequencies followed by clustering (Materials and Methods). Shown are the results from positive correlation at low and negative correlation at high frequency. (B) Heat map displaying change in physical, biological and chemical environmental parameters over the time series. Color scale for each environmental parameter varies between maximum and minimum values, which are for each parameter: WWTMP: 20-10 ºC; ATMP: 30-10 ºC; DWD: 14-4 s, WS: 14-4 m/s; WL: 4.5-1.5 m; WH: 3-0.5 m; Press: 1020-995 hPa; TD: 1-0 incoming/outgoing; Malgae: 4-0 relative concentration; CCon: 10-4 µg/L; NH_4: 1.4-0 µM; NO_2-NO_3: 20-0 µM; PO_4: 0.7-0 µM; Silicate: 10-2 µM; Salinity: 36-33 psu. For more details see Supplementary Data 7 where values for each day are listed. Day 247, which marks hurricane Earl passage, is framed in the heat map. (C) Granger causalities linking predicted communities to each other and to environmental parameters. Nodes represent communities (colored according to panel A) and environmental parameters (grey). Legends for B and C: WTMP, water temperature; ATMP, air temperature; DWD, dominant wave period; WS, wind speed; WL, water level; WH, wave height; Press,

pressure; TD, tidal direction; Malgae, macroalgae; CCon, Chlorophyll concentration; NH_4, ammonium; NO_2-NO_3, nitrite and nitrates; PO_4, phosphate.

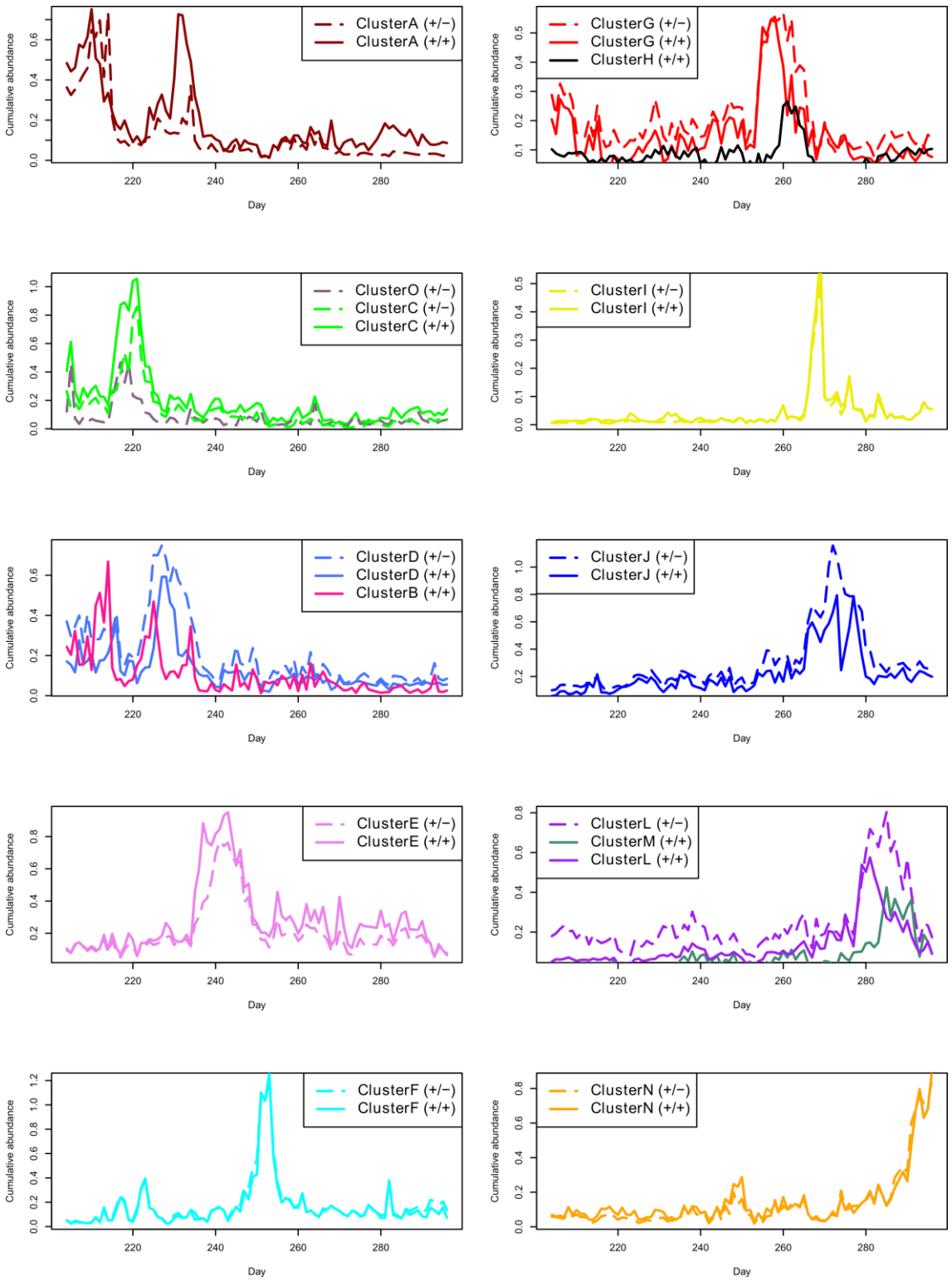

Supplementary Fig. 4 | Direct comparison of communities predicted by positive correlations at low frequency with either positive (solid line) or negative (dashed line) interactions at high frequency. Although there is generally high agreement between +/+ and +/- correlations, some exceptions emerge. For example, cluster C (+/+) approximately splits in two clusters, C and O, when considering +/- correlations. Similarly, cluster D and L in +/- correlations approximately split in two clusters (D and B, and L and M, respectively) when considering +/+ correlations. Color-coding according to communities shown in Fig. 2.

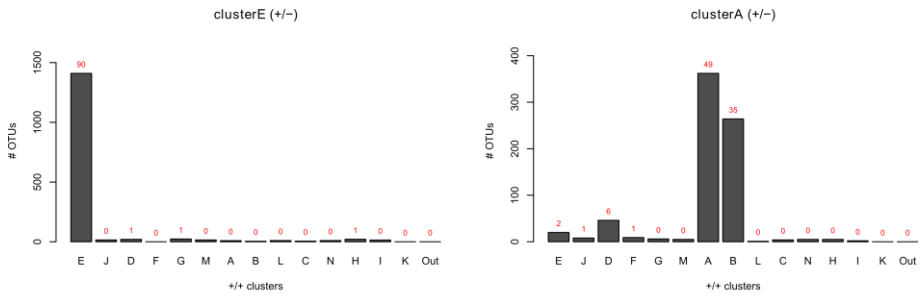
clusterE (+/−)
OTUs
+/+ clusters
E J D F G M A B L C N H I K Out
90 0 1 0 1 0 0 0 0 0 0 1 0 0 0

clusterA (+/−)
OTUs
+/+ clusters
E J D F G M A B L C N H I K Out
2 1 6 1 0 0 49 35 0 0 0 0 0 0 0

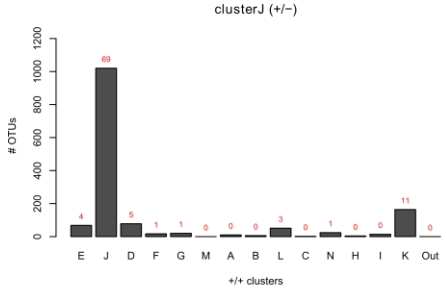
clusterJ (+/−)
OTUs
+/+ clusters
E J D F G M A B L C N H I K Out
4 89 5 1 1 0 0 0 3 0 1 0 0 11 0

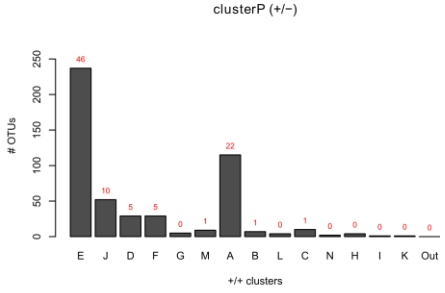
clusterP (+/−)
OTUs
+/+ clusters
E J D F G M A B L C N H I K Out
46 10 5 5 0 1 22 1 0 1 0 0 0 0 0

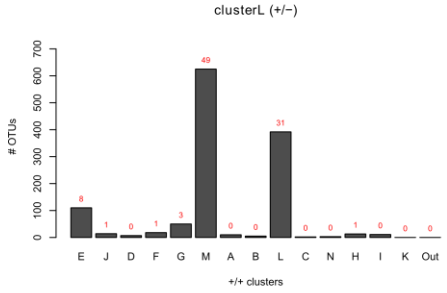
clusterL (+/−)
OTUs
+/+ clusters
E J D F G M A B L C N H I K Out
8 1 0 1 3 49 0 0 31 0 0 1 0 0 0

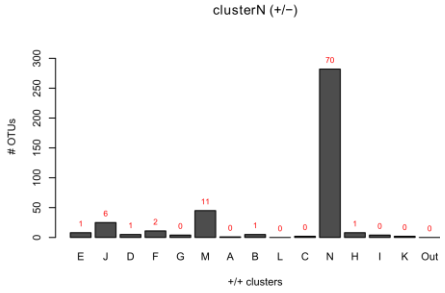
clusterN (+/−)
OTUs
+/+ clusters
E J D F G M A B L C N H I K Out
1 6 1 2 0 11 0 1 0 0 70 1 0 0 0

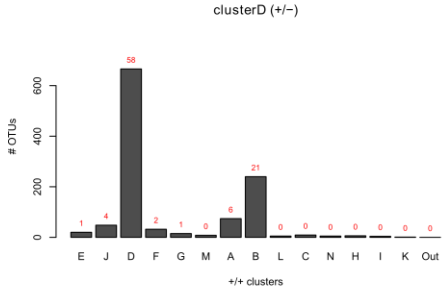
clusterD (+/−)
OTUs
+/+ clusters
E J D F G M A B L C N H I K Out
1 4 58 2 1 0 6 21 0 0 0 0 0 0 0

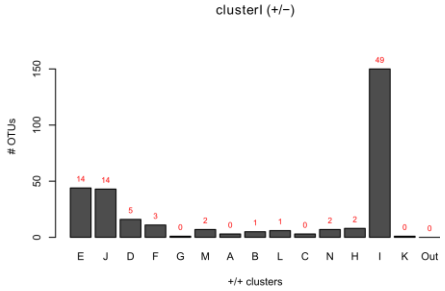
clusterI (+/−)
OTUs
+/+ clusters
E J D F G M A B L C N H I K Out
14 14 5 3 0 2 0 1 1 0 2 2 49 0 0

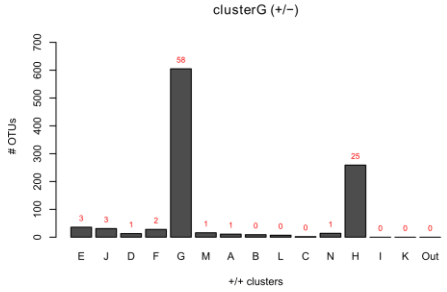
clusterG (+/−)
OTUs
+/+ clusters
E J D F G M A B L C N H I K Out
3 3 1 2 58 1 1 0 0 0 1 25 0 0 0

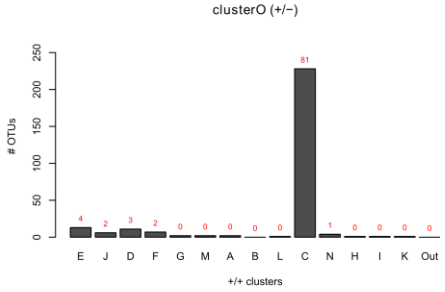
clusterO (+/−)
OTUs
+/+ clusters
E J D F G M A B L C N H I K Out
4 2 3 2 0 0 0 0 0 81 1 0 0 0 0

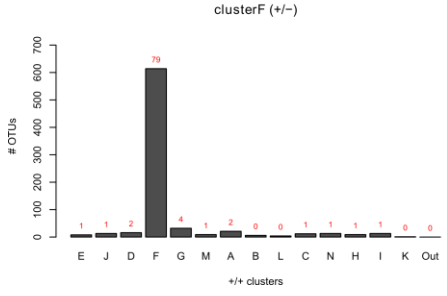
clusterF (+/−)
OTUs
+/+ clusters
E J D F G M A B L C N H I K Out
1 1 2 79 4 1 2 0 1 1 1 1 0 0

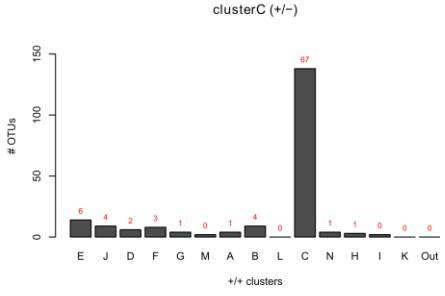
clusterC (+/−)
OTUs
+/+ clusters
E J D F G M A B L C N H I K Out
6 4 2 3 1 0 1 4 0 67 1 1 0 0 0

Supplementary Figure 5 | Number of OTUs shared among clusters defined by negative and positive high frequency interactions. For each cluster defined by negative high frequency interactions, shown is the percentage overlap in OTUs with each of the clusters defined by positive high frequency interaction ($\frac{\#intersecting\ OTUs}{total\ OTUs\ in\ cluster}$). Assigning similar clusters with more than a 65% overlap, we found that 6 out of 12 negative interaction clusters were also directly found among the positive interaction clusters, while the remaining 6 were mainly split in two of the positive clusters (both summing up more than this 65% overlap).

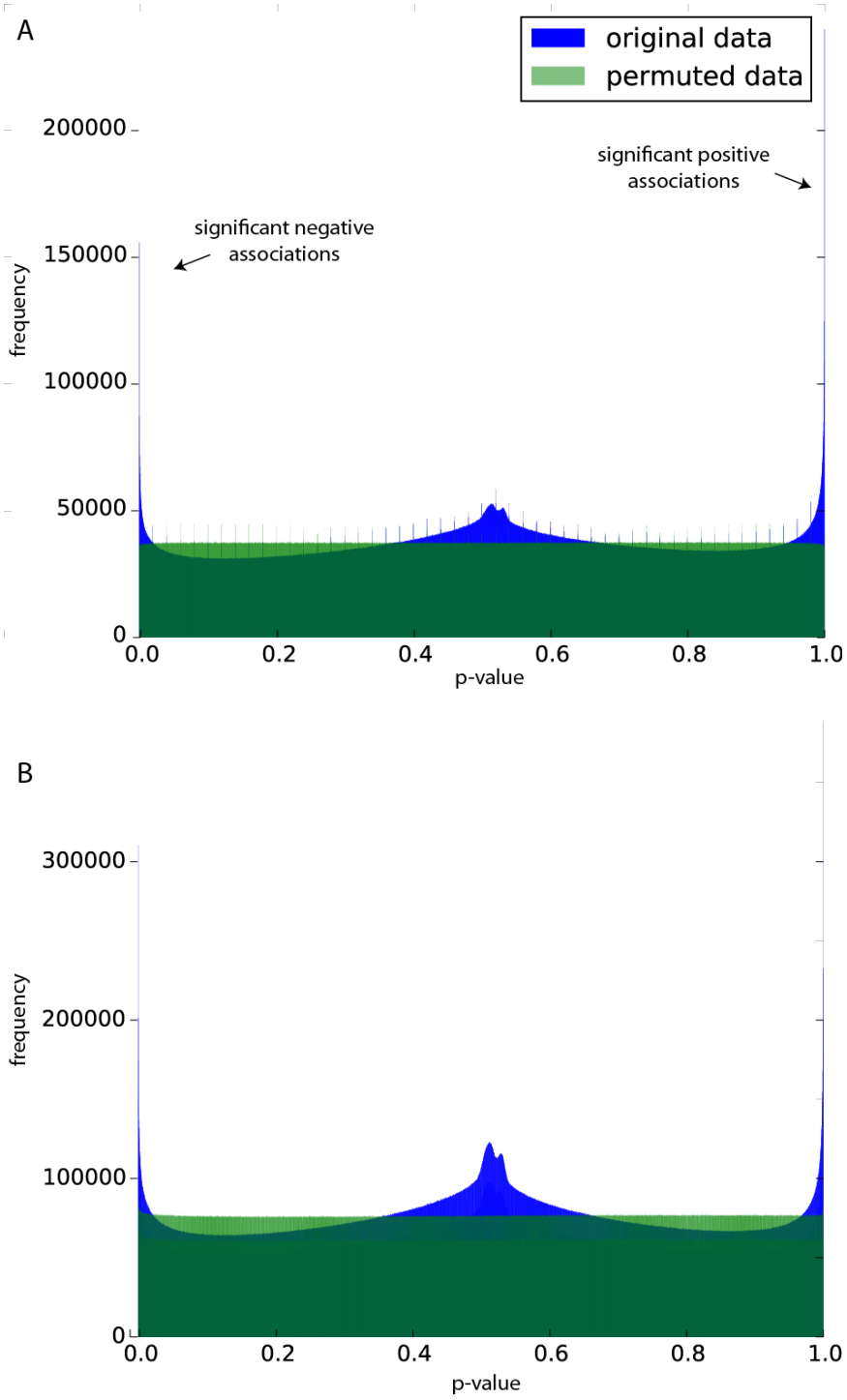

Supplementary Fig. 6 | Significant positive and negative WaveClust associations identified by permutation analysis. Permuted time series were used to calculate empirical p-values in **(A)** distributional OTU time series (original data) and **(B)** non-distributional (100% sequence identity) time series. Green histograms depict the distribution of p-values found in randomly shuffled data. Blue histograms depict the distribution of p-values in real data. Real data are enriched for significant positive (p-values close to 1) and negative associations (p-values close to 0) at a similar frequency in **(A)** and **(B)**.

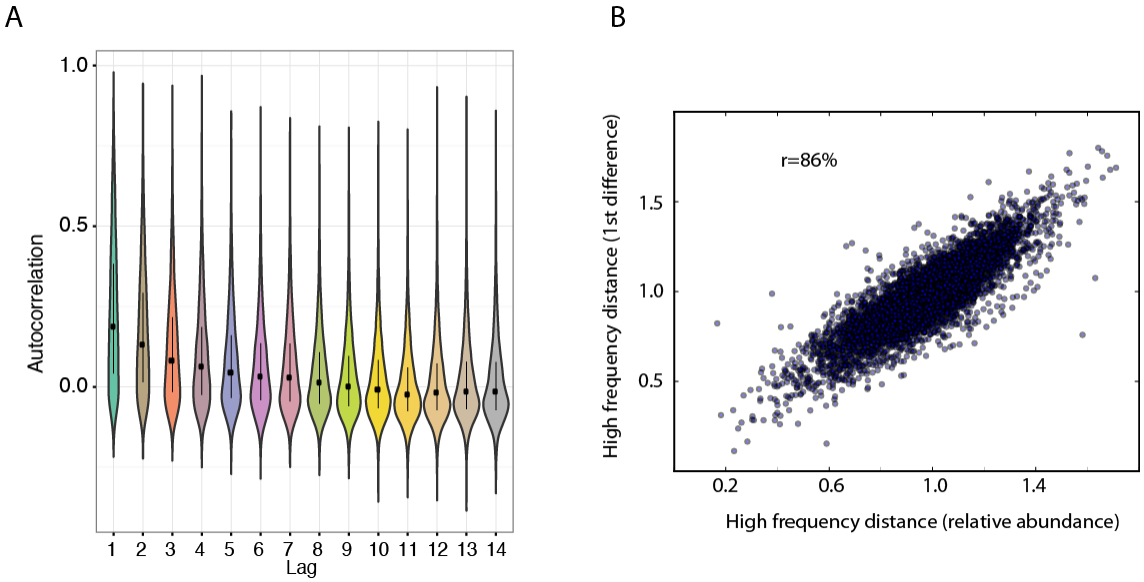

Supplementary Fig. 7 | Autocorrelation has little effect on WaveClust similarity. **(A)** Autocorrelation levels (Y axis) were calculated for each time series at a lag of 1 to 14 days (X axis). Violin plots depict the distribution of autocorrelation values at each time lag (dots represent median; bars represent interquartile range). Autocorrelation at a 1-day lag was removed by calculating the 1st difference for each time series. **(B)** High-frequency similarity scores calculated from the original data (X axis) are highly correlated (86% Pearson correlation) with high-frequency similarity scores calculated from 1st different data (Y axis; each dot represents one OTU time series).

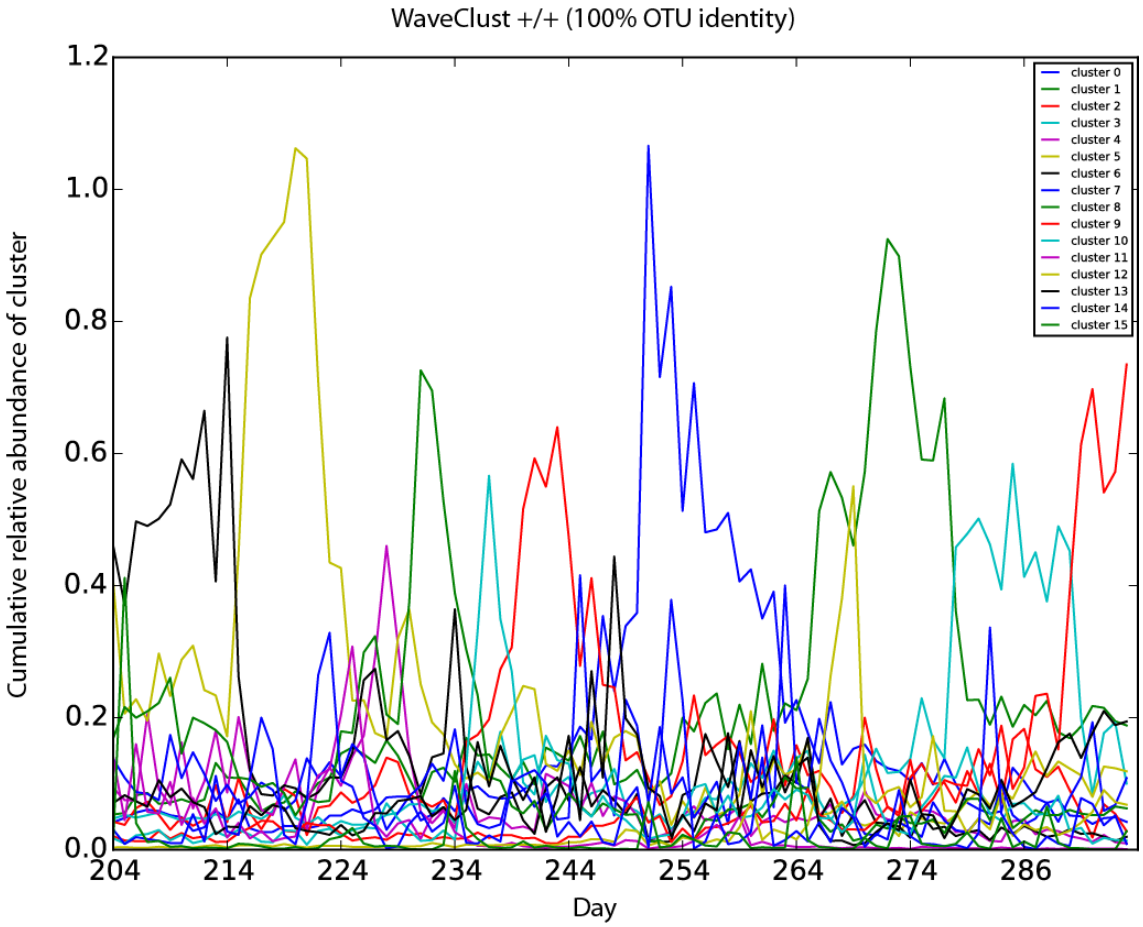

Supplementary Fig. 8 | WaveClust clustering of non-distributional OTUs collapsed at 100% sequence identity. OTUs were defined at 100% sequence identity to create an alternative dataset to distributional OTUs. Plot depicts cumulative abundance time series of non-distributional OTU clusters found by WaveClust. WaveClust scores were generated using positive correlations at high- and low-frequency (similar results were obtained with negative correlations at high-frequency; data not shown). Permutation analysis was used to keep only those scores passing a false discovery rate of 10%. The number of clusters, timing of cluster peaks, and sharp transitions are similar to results found with distributional OTUs.

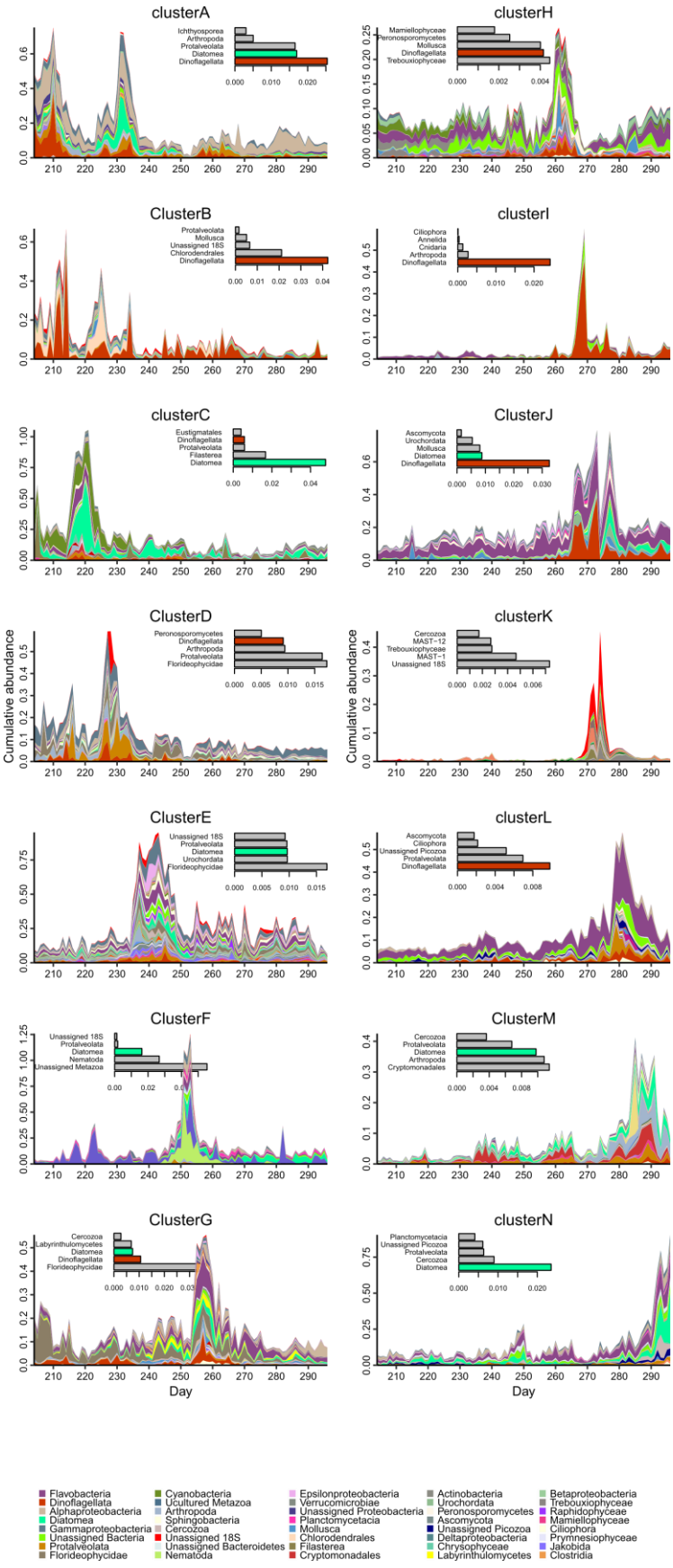

Supplementary Fig. 9 | Taxonomic groups with highest relative frequencies in the most abundant communities. Inset bargraphs show the average relative abundance of

the 5 most prevalent eukaryotic groups highlighting alternating dominance of dinoflagellates (orange-red) and diatoms (spring-green) as primary producers. Legends for class-level taxa are ordered from most to least abundant for the 40 most overall abundant classes (the remaining low abundant classes are omitted in the legend).

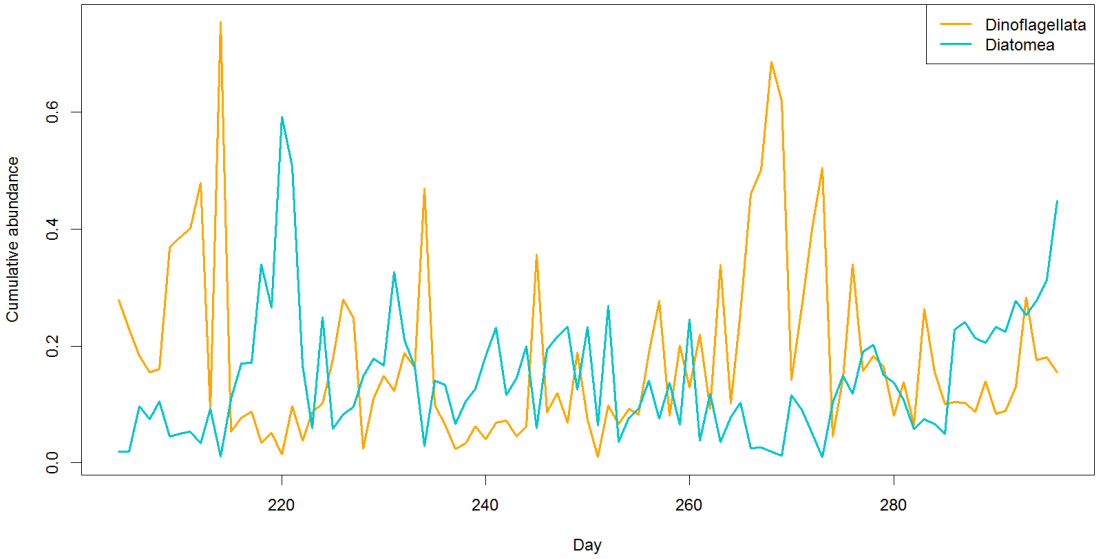

Supplementary Fig. 10 | Alternating dominance of diatoms and dinoflagellates in the time series. Changes in relative abundance are shown for Diatomea and Dinoflagellata, i.e. the sum of all diatom and dinoflagellate OTUs, respectively.

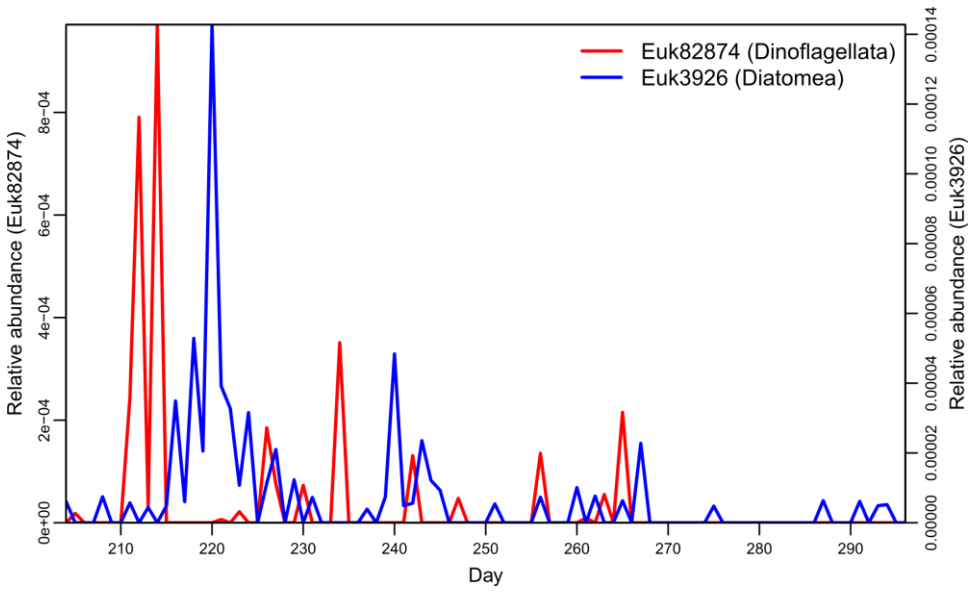

Supplementary Fig. 11 | Example of taxonomically highly resolved alternating shifts in dominance among dinoflagellate and diatom. Shown are changes in relative abundance among one diatom and one dinoflagellate OTU.

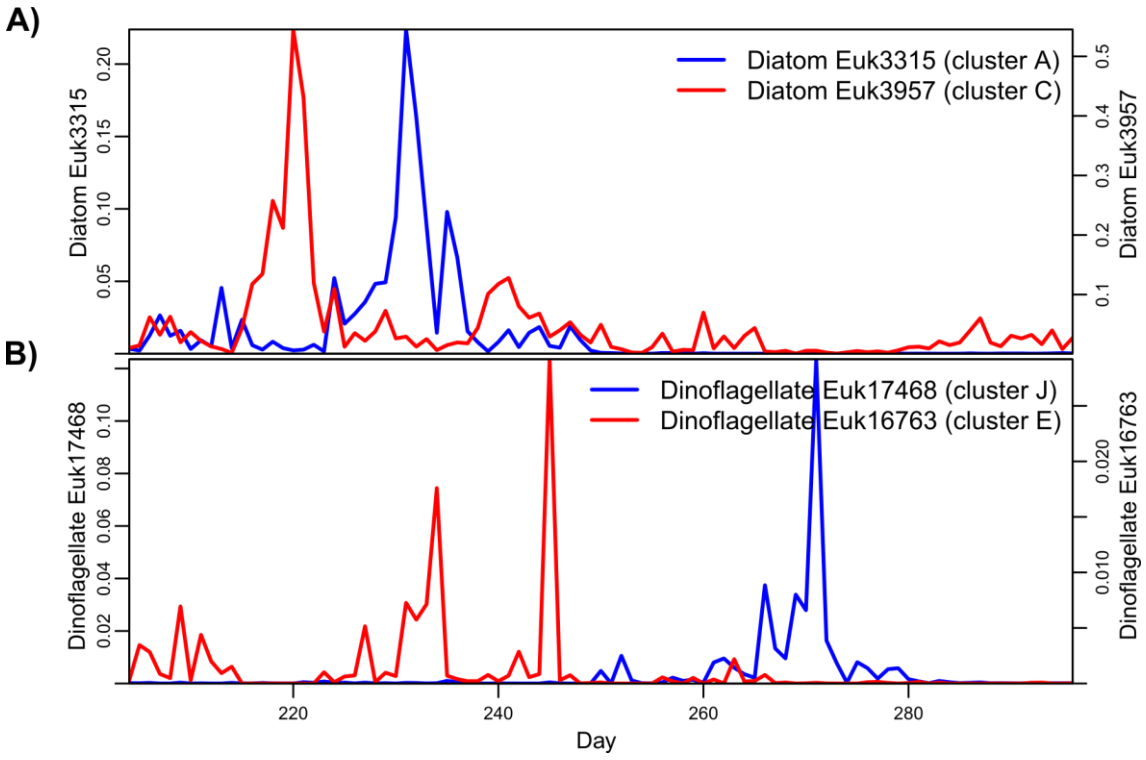

Supplementary Fig. 12 | Different diatom and dinoflagellate OTUs peak in different communities. Example of daily dynamics of some diatoms (A) and dinoflagellate (B) OTUs, each reaching highest relative abundance within different community clusters.

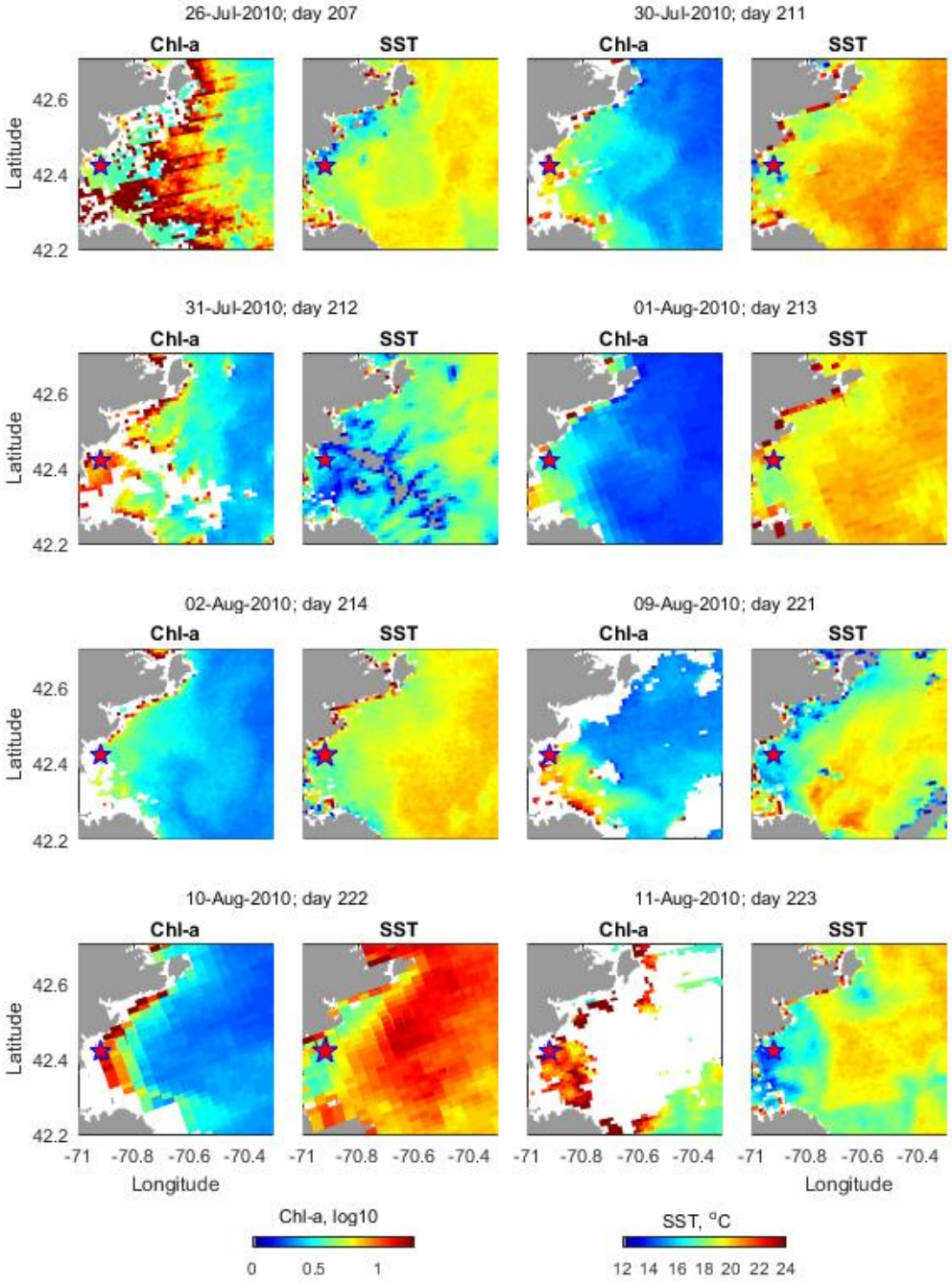
26-Jul-2010; day 207
30-Jul-2010; day 211
31-Jul-2010; day 212
01-Aug-2010; day 213
02-Aug-2010; day 214
09-Aug-2010; day 221
10-Aug-2010; day 222
11-Aug-2010; day 223
Chl-a
SST
Latitude
42.6
42.4
42.2
-71
-70.8
-70.6
-70.4
Longitude
Chl-a, log10
0
0.5
1
SST, °C
12 14 16 18 20 22 24

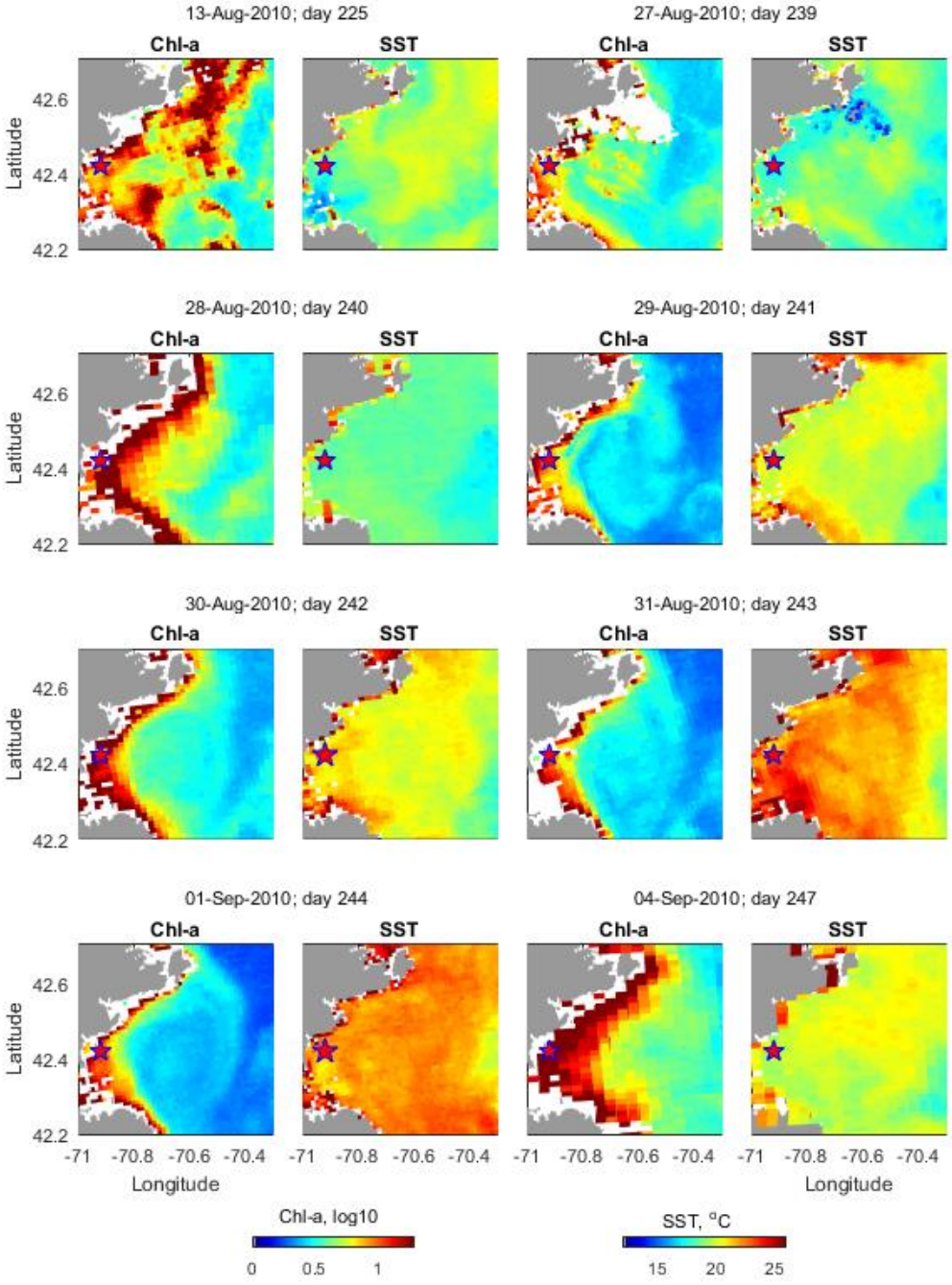
13-Aug-2010; day 225
27-Aug-2010; day 239
28-Aug-2010; day 240
29-Aug-2010; day 241
30-Aug-2010; day 242
31-Aug-2010; day 243
01-Sep-2010; day 244
04-Sep-2010; day 247
Chl-a
SST
Latitude
42.6
42.4
42.2
-71
-70.8
-70.6
-70.4
Longitude
Chl-a, log10
0
0.5
1
SST, °C
15
20
25

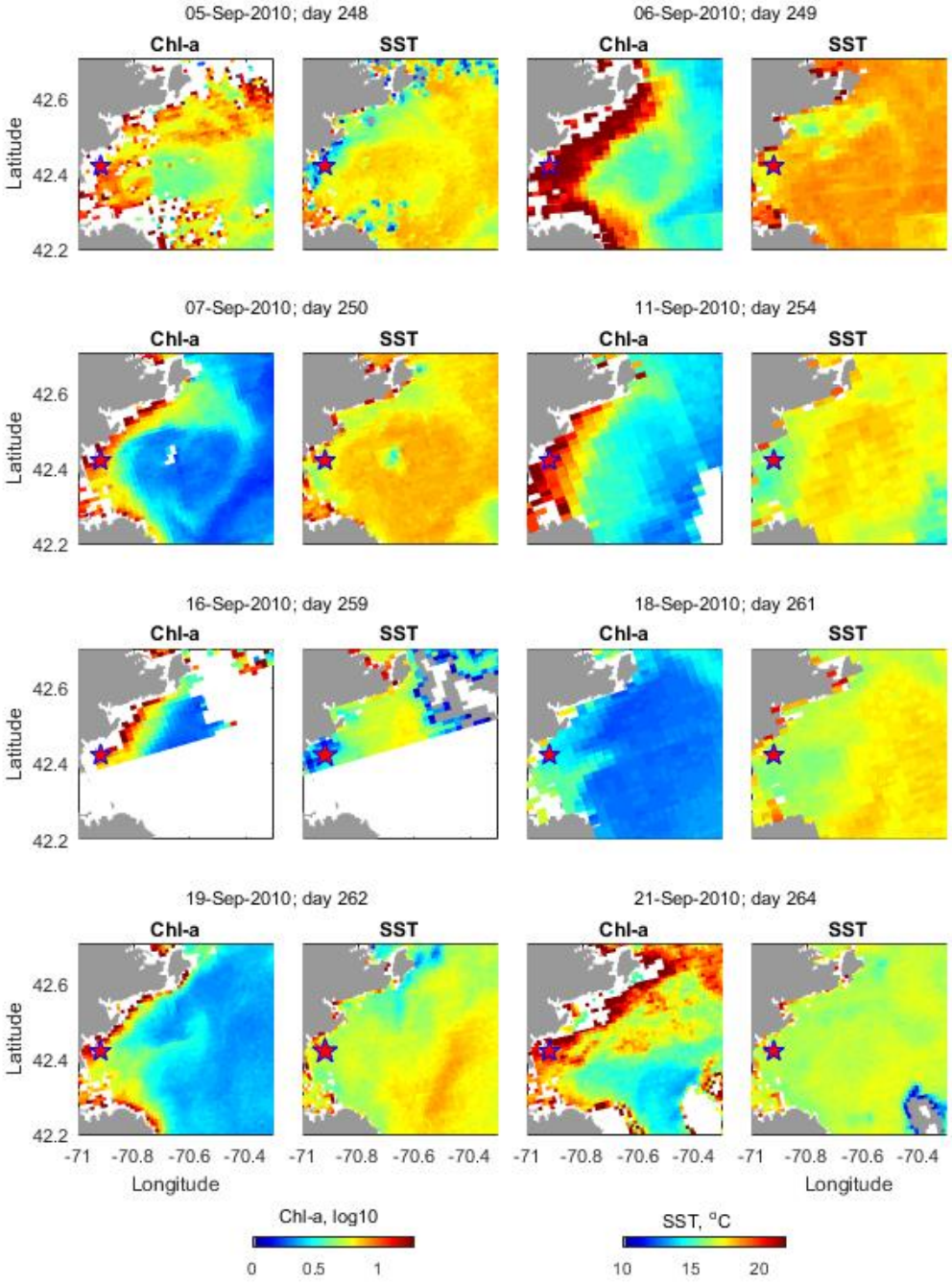
05-Sep-2010; day 248
Chl-a
SST
06-Sep-2010; day 249
Chl-a
SST
07-Sep-2010; day 250
Chl-a
SST
11-Sep-2010; day 254
Chl-a
SST
16-Sep-2010; day 259
Chl-a
SST
18-Sep-2010; day 261
Chl-a
SST
19-Sep-2010; day 262
Chl-a
SST
21-Sep-2010; day 264
Chl-a
SST
Latitude
42.6
42.4
42.2
-71
-70.8
-70.6
-70.4
Longitude
Chl-a, log10
0
0.5
1
SST, °C
10
15
20

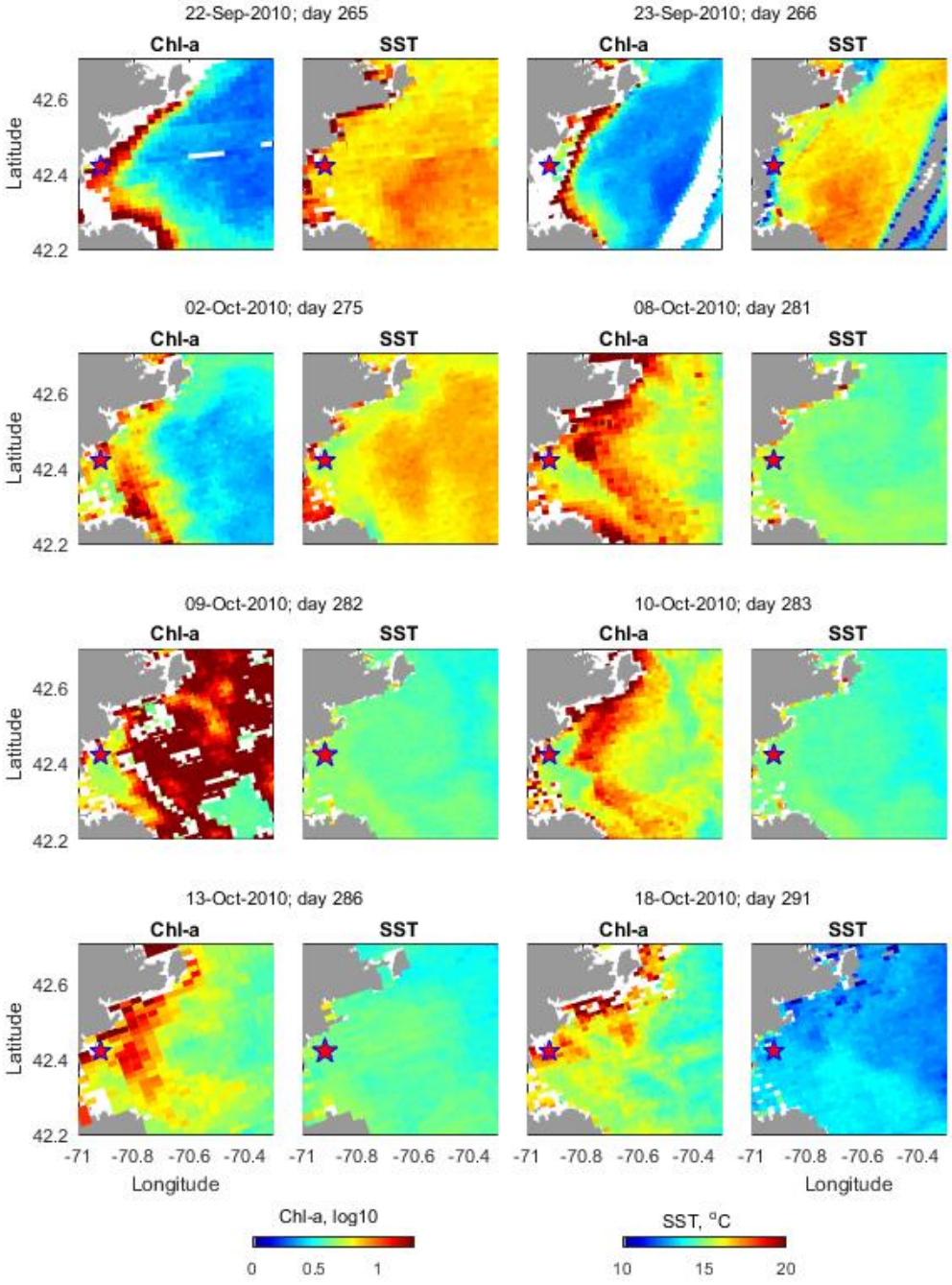
22-Sep-2010; day 265
23-Sep-2010; day 266
02-Oct-2010; day 275
08-Oct-2010; day 281
09-Oct-2010; day 282
10-Oct-2010; day 283
13-Oct-2010; day 286
18-Oct-2010; day 291
Chl-a
SST
Latitude
42.6
42.4
42.2
-71
-70.8
-70.6
-70.4
Longitude
Chl-a, log10
0
0.5
1
SST, °C
10
15
20

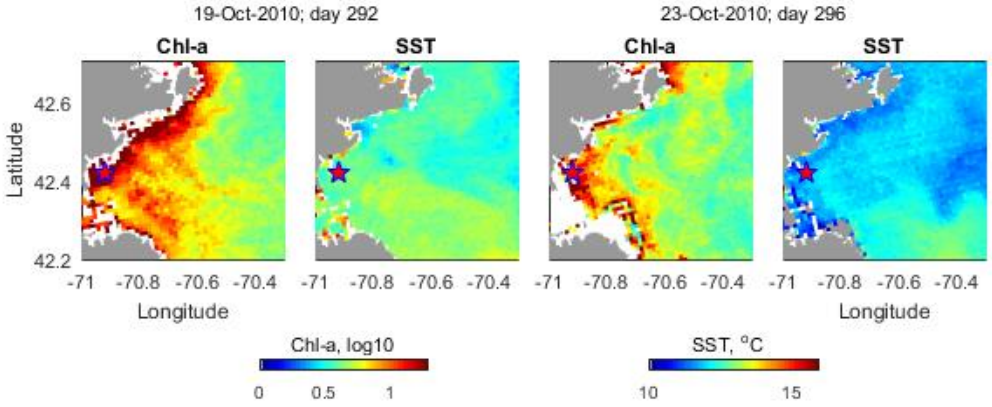

Supplementary Fig. 13 | Time-series of chlorophyll *a* (Chl-a) and sea surface temperature (SST). Data are from MODIS-A satellite imagery for the period 26 July to 23 October 2010. Only relatively cloud-free scenes are shown. Compare to Supplementary Fig. 4 for comparison of temporal dynamics of communities.

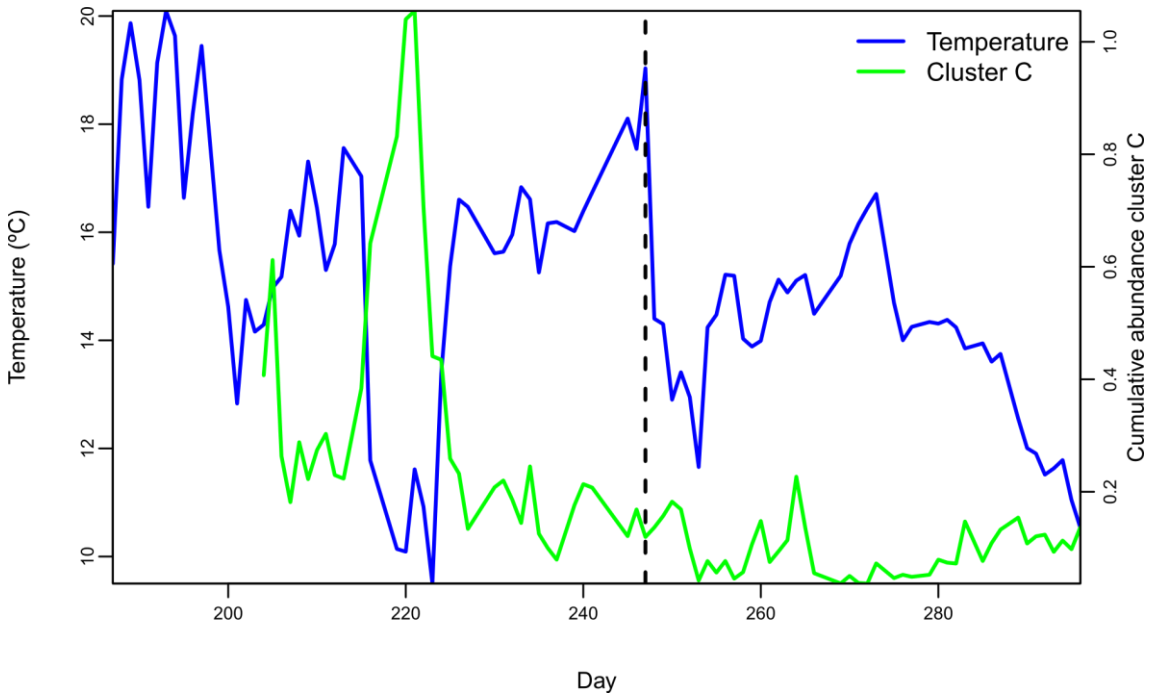

Supplementary Fig. 14 | Dynamics of community cluster C and temperature variation. Cluster C defined by positive correlations at low and high frequencies shows its highest expansion during cold water intrusion and consideration of temperature values preceding the time series sampling suggests that the slight peak at the beginning of the time series might have happened during another cold water period not captured by the biological sampling in this time series. Vertical dashed line highlights day 247, marking the passage of hurricane Earl.

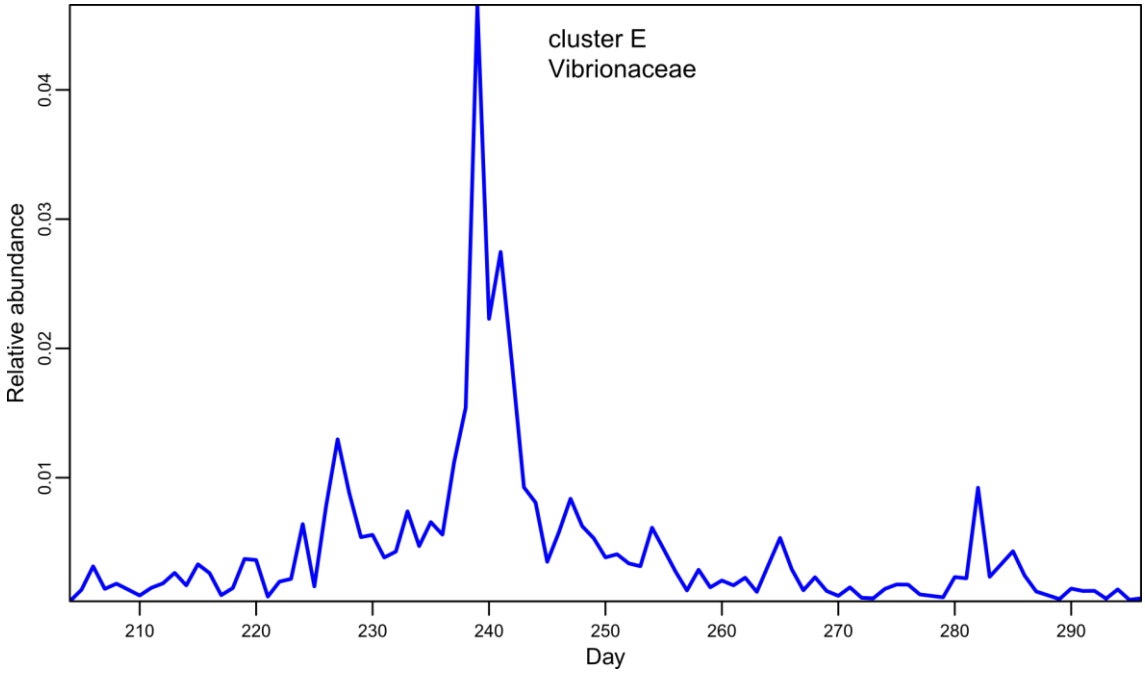

Supplementary Fig. 15 | Vibrionaceae bloom in community E. The bloom occurred during a period characterized by warm water and abundant macroalgal detritus. See Fig. 2 for details on community dynamics.

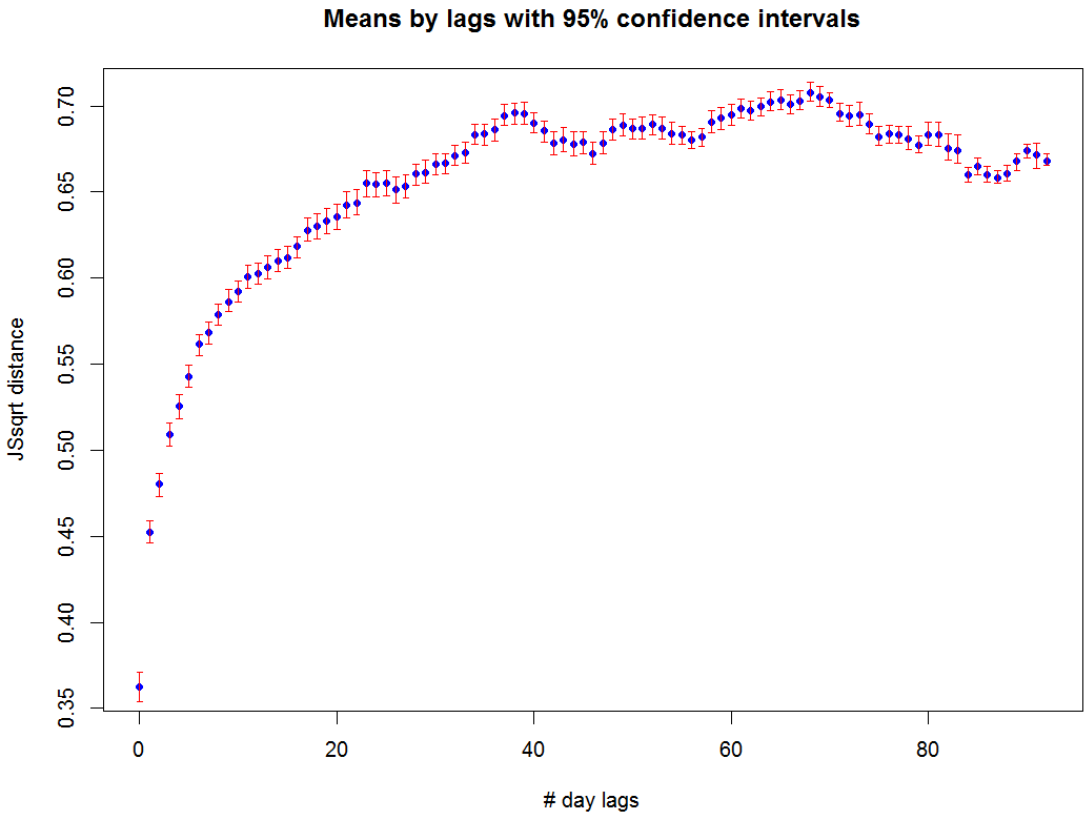

Supplementary Fig. 16 | Jensen-Shannon square root distance between samples for different time-lags. Replicates (lag 0) are most closely related.

Supplementary Table 1. Clusters estimated by WaveClust and associated numbers of OTUs.

	WaveClust	
Cluster	+/+ (Fig. 2)	+/- (Fig. S3)
A	622	737
B	560	ND
C	417	203
D	913	1133
E	1988	1556
F	784	771
G	767	1031
H	341	ND
I	216	305
J	1284	1478
K	171	ND
L	481	1260
M	743	ND
N	373	402
O	ND	279
P	ND	505

ND = cluster not detected.

Supplementary Table 2. Sample-specific barcode sequences.

Barcode ID	Barcode sequence	96-well position
001	TCCGTGCGC	A1
002	TGTTTCCCA	A2
003	GGTAATGAA	A3
004	GAAACTGGG	A4
005	ACGGGCTGA	A5
006	ATGAAGTAT	A6
007	ACTTATTGT	A7
008	GGCGGGAAA	A8
009	ACACCTCGG	A9
010	CTCATTGGG	A10
011	GCTGCCGCG	A11
012	CGATGGTGT	A12
013	TCAAAGCTG	B1
014	CAGCGGCAT	B2
015	CCGACAAAT	B3
016	TAAGGGAGA	B4
017	TTGTGGCGC	B5
018	AGGTCGGTC	B6
019	AATGTCAAG	B7
020	GTTCGCAGG	B8
021	TATCAATCT	B9
022	GTCTAACGC	B10
023	TTACTATAC	B11
024	TGCACCCGT	B12
025	TGGGACCTC	C1
026	GAGTTTGAT	C2
027	AACAGTATT	C3
028	ATCGCACCA	C4
029	CTAGAATCT	C5
030	CGCCAAGGG	C6
031	AGTATGCAG	C7
032	CCTTTGATA	C8
033	TTTAACTGA	C9
034	CTTGCTTGG	C10
035	TCGGCTCGG	C11
036	CAAGCCTGC	C12
037	ATAGGTGGA	D1
038	CAACTTCAT	D2
039	GTAGTCGAG	D3
040	TCCCGATGA	D4
041	GGGCGAAAT	D5
042	GCGTAGGAT	D6
043	GGCCTCGCC	D7
044	GGTGTACCA	D8
045	CCCAGGCAG	D9
046	GTCACGGGA	D10
047	AATACAGGT	D11
048	TATTCTGTA	D12
049	CGTCCCACC	E1
050	CTGTTAGTC	E2
051	CACTCACTA	E3

052	ACCTCCCAT	E4
053	GAGCACAGG	E5
054	CGGAGTGCT	E6
055	GCAAGATAC	E7
056	CGAATATTC	E8
057	AAGGAACGT	E9
058	GATTGAAGT	E10
059	TGATAATAT	E11
060	CCACGCAAG	E12
061	TACGATACT	F1
062	AGGCTTCAT	F2
063	GTGCTGATC	F3
064	ACCATACTA	F4
065	AAATTGGAC	F5
066	TAGAGCCAA	F6
067	TTATCCTTG	F7
068	TTCCAGATG	F8
069	CACAACGAA	F9
070	AACCCGTTG	F10
071	CTACCGATG	F11
072	GTGGATAGC	F12
073	GCCTGTTCC	G1
074	AGCTGACGG	G2
075	AGAGAGGCT	G3
076	GCAATGGAT	G4
077	TGACTTAGC	G5
078	AAACAAGAT	G6
079	CTTCAGCTG	G7
080	GGAGGCTGT	G8
081	ACAAACTAC	G9
082	GACATCATA	G10
083	AGTCACCCG	G11
084	TCTAGTCGT	G12
085	CCGCACCGA	H1
086	ATGCCAGCA	H2
087	TCGAACACA	H3
088	CGACATTCA	H4
089	CATCGCTAG	H5
090	AAATCATTA	H6
091	TCTGTATGT	H7
092	ACTAAGATA	H8
093	CCCGTTTCA	H9
094	GTACGTTGC	H10
095	AGTAGATGA	H11
096	TCATTAAGG	H12

Supplementary Table 3. Sequencing platform used for each sample.

Sample	rRNA gene sequenced	Sequencing platform
10N.204.37	16S	Illumina MiSeq
10N.204.38	16S	Illumina MiSeq
10N.204.39	16S	Illumina MiSeq
10N.205.37	16S	Illumina MiSeq
10N.205.38	16S	Illumina MiSeq
10N.205.39	16S	Illumina MiSeq
10N.206.37	16S	Illumina MiSeq
10N.206.38	16S	Illumina MiSeq
10N.206.39	16S	Illumina MiSeq
10N.207.37	16S	Illumina MiSeq
10N.207.38	16S	Illumina MiSeq
10N.207.39	16S	Illumina MiSeq
10N.208.37	16S	Illumina MiSeq
10N.208.38	16S	Illumina MiSeq
10N.208.39	16S	Illumina MiSeq
10N.209.37	16S	Illumina MiSeq
10N.209.38	16S	Illumina MiSeq
10N.209.39	16S	Illumina MiSeq
10N.210.37	16S	Illumina MiSeq
10N.210.38	16S	Illumina MiSeq
10N.210.39	16S	Illumina MiSeq
10N.211.37	16S	Illumina MiSeq
10N.211.38	16S	Illumina MiSeq
10N.211.39	16S	Illumina MiSeq
10N.212.37	16S	Illumina MiSeq
10N.212.38	16S	Illumina MiSeq
10N.212.39	16S	Illumina MiSeq
10N.213.37	16S	Illumina MiSeq
10N.213.38	16S	Illumina MiSeq
10N.213.39	16S	Illumina MiSeq
10N.214.37	16S	Illumina MiSeq
10N.214.38	16S	Illumina MiSeq
10N.214.39	16S	Illumina MiSeq
10N.215.37	16S	Illumina MiSeq
10N.215.38	16S	Illumina MiSeq
10N.215.39	16S	Illumina MiSeq
10N.216.37	16S	Illumina MiSeq
10N.216.38	16S	Illumina MiSeq
10N.216.39	16S	Illumina MiSeq
10N.217.37	16S	Illumina MiSeq
10N.217.38	16S	Illumina MiSeq
10N.217.39	16S	Illumina MiSeq
10N.218.37	16S	Illumina MiSeq

10N.218.38	16S	Illumina MiSeq
10N.218.39	16S	Illumina MiSeq
10N.219.37	16S	Illumina MiSeq
10N.219.38	16S	Illumina MiSeq
10N.219.39	16S	Illumina MiSeq
10N.220.37	16S	Illumina MiSeq
10N.220.38	16S	Illumina MiSeq
10N.220.39	16S	Illumina MiSeq
10N.221.37	16S	Illumina MiSeq
10N.221.38	16S	Illumina MiSeq
10N.221.39	16S	Illumina MiSeq
10N.222.37	16S	Illumina MiSeq
10N.222.38	16S	Illumina MiSeq
10N.222.39	16S	Illumina MiSeq
10N.223.37	16S	Illumina MiSeq
10N.223.38	16S	Illumina MiSeq
10N.223.39	16S	Illumina MiSeq
10N.224.37	16S	Illumina MiSeq
10N.224.38	16S	Illumina MiSeq
10N.224.39	16S	Illumina MiSeq
10N.225.37	16S	Illumina MiSeq
10N.225.38	16S	Illumina MiSeq
10N.225.39	16S	Illumina MiSeq
10N.226.37	16S	Illumina MiSeq
10N.226.38	16S	Illumina MiSeq
10N.226.39	16S	Illumina MiSeq
10N.227.37	16S	Illumina MiSeq
10N.227.38	16S	Illumina MiSeq
10N.227.39	16S	Illumina MiSeq
10N.228.37	16S	Illumina MiSeq
10N.228.38	16S	Illumina MiSeq
10N.228.39	16S	Illumina MiSeq
10N.229.37	16S	Illumina MiSeq
10N.229.38	16S	Illumina MiSeq
10N.229.39	16S	Illumina MiSeq
10N.230.37	16S	Illumina MiSeq
10N.230.38	16S	Illumina MiSeq
10N.230.39	16S	Illumina MiSeq
10N.231.37	16S	Illumina MiSeq
10N.231.38	16S	Illumina MiSeq
10N.231.39	16S	Illumina MiSeq
10N.232.37	16S	Illumina MiSeq
10N.232.38	16S	Illumina MiSeq
10N.232.39	16S	Illumina MiSeq
10N.233.37	16S	Illumina MiSeq
10N.233.38	16S	Illumina MiSeq
10N.233.39	16S	Illumina MiSeq
10N.234.37	16S	Illumina MiSeq

10N.234.38	16S	Illumina MiSeq
10N.234.39	16S	Illumina MiSeq
10N.235.37	16S	Illumina MiSeq
10N.235.38	16S	Illumina MiSeq
10N.235.39	16S	Illumina HiSeq 1000
10N.236.37	16S	Illumina HiSeq 1000
10N.236.38	16S	Illumina HiSeq 1000
10N.236.39	16S	Illumina HiSeq 1000
10N.237.37	16S	Illumina HiSeq 1000
10N.237.38	16S	Illumina HiSeq 1000
10N.237.39	16S	Illumina HiSeq 1000
10N.238.37	16S	Illumina HiSeq 1000
10N.238.38	16S	Illumina HiSeq 1000
10N.238.39	16S	Illumina HiSeq 1000
10N.239.37	16S	Illumina HiSeq 1000
10N.239.38	16S	Illumina HiSeq 1000
10N.239.39	16S	Illumina HiSeq 1000
10N.240.37	16S	Illumina HiSeq 1000
10N.240.38	16S	Illumina HiSeq 1000
10N.240.39	16S	Illumina HiSeq 1000
10N.241.37	16S	Illumina HiSeq 1000
10N.241.38	16S	Illumina HiSeq 1000
10N.241.39	16S	Illumina HiSeq 1000
10N.242.37	16S	Illumina HiSeq 1000
10N.242.38	16S	Illumina HiSeq 1000
10N.242.39	16S	Illumina HiSeq 1000
10N.243.37	16S	Illumina HiSeq 1000
10N.243.38	16S	Illumina HiSeq 1000
10N.243.39	16S	Illumina HiSeq 1000
10N.244.37	16S	Illumina HiSeq 1000
10N.244.38	16S	Illumina HiSeq 1000
10N.244.39	16S	Illumina HiSeq 1000
10N.245.37	16S	Illumina HiSeq 1000
10N.245.38	16S	Illumina HiSeq 1000
10N.245.39	16S	Illumina HiSeq 1000
10N.246.37	16S	Illumina HiSeq 1000
10N.246.38	16S	Illumina HiSeq 1000
10N.246.39	16S	Illumina HiSeq 1000
10N.247.37	16S	Illumina HiSeq 1000
10N.247.38	16S	Illumina HiSeq 1000
10N.247.39	16S	Illumina HiSeq 1000
10N.248.37	16S	Illumina HiSeq 1000
10N.248.38	16S	Illumina HiSeq 1000
10N.248.39	16S	Illumina HiSeq 1000
10N.249.37	16S	Illumina HiSeq 1000
10N.249.38	16S	Illumina HiSeq 1000
10N.249.39	16S	Illumina HiSeq 1000
10N.250.37	16S	Illumina HiSeq 1000

10N.250.38	16S	Illumina HiSeq 1000
10N.250.39	16S	Illumina HiSeq 1000
10N.251.37	16S	Illumina HiSeq 1000
10N.251.38	16S	Illumina HiSeq 1000
10N.251.39	16S	Illumina HiSeq 1000
10N.252.37	16S	Illumina HiSeq 1000
10N.252.38	16S	Illumina HiSeq 1000
10N.252.39	16S	Illumina HiSeq 1000
10N.253.37	16S	Illumina HiSeq 1000
10N.253.38	16S	Illumina HiSeq 1000
10N.253.39	16S	Illumina HiSeq 1000
10N.254.37	16S	Illumina HiSeq 1000
10N.254.38	16S	Illumina HiSeq 1000
10N.254.39	16S	Illumina HiSeq 1000
10N.255.37	16S	Illumina HiSeq 1000
10N.255.38	16S	Illumina HiSeq 1000
10N.255.39	16S	Illumina HiSeq 1000
10N.256.37	16S	Illumina HiSeq 1000
10N.256.38	16S	Illumina HiSeq 1000
10N.256.39	16S	Illumina HiSeq 1000
10N.257.37	16S	Illumina HiSeq 1000
10N.257.38	16S	Illumina HiSeq 1000
10N.257.39	16S	Illumina HiSeq 1000
10N.258.37	16S	Illumina HiSeq 1000
10N.258.38	16S	Illumina HiSeq 1000
10N.258.39	16S	Illumina HiSeq 1000
10N.259.37	16S	Illumina HiSeq 1000
10N.259.38	16S	Illumina HiSeq 1000
10N.259.39	16S	Illumina HiSeq 1000
10N.260.37	16S	Illumina HiSeq 1000
10N.260.38	16S	Illumina HiSeq 1000
10N.260.39	16S	Illumina HiSeq 1000
10N.261.37	16S	Illumina HiSeq 1000
10N.261.38	16S	Illumina HiSeq 1000
10N.261.39	16S	Illumina HiSeq 1000
10N.262.37	16S	Illumina HiSeq 1000
10N.262.38	16S	Illumina HiSeq 1000
10N.262.39	16S	Illumina HiSeq 1000
10N.263.37	16S	Illumina HiSeq 1000
10N.263.38	16S	Illumina HiSeq 1000
10N.263.39	16S	Illumina HiSeq 1000
10N.264.37	16S	Illumina HiSeq 1000
10N.264.38	16S	Illumina HiSeq 1000
10N.264.39	16S	Illumina HiSeq 1000
10N.265.37	16S	Illumina HiSeq 1000
10N.265.38	16S	Illumina HiSeq 1000
10N.265.39	16S	Illumina HiSeq 1000
10N.266.37	16S	Illumina HiSeq 1000

10N.266.38	16S	Illumina HiSeq 1000
10N.266.39	16S	Illumina HiSeq 1000
10N.267.37	16S	Illumina HiSeq 1000
10N.267.38	16S	Illumina HiSeq 1000
10N.267.39	16S	Illumina HiSeq 1000
10N.268.37	16S	Illumina HiSeq 1000
10N.268.38	16S	Illumina HiSeq 1000
10N.268.39	16S	Illumina HiSeq 1000
10N.269.37	16S	Illumina HiSeq 1000
10N.269.38	16S	Illumina HiSeq 1000
10N.269.39	16S	Illumina HiSeq 1000
10N.270.37	16S	Illumina HiSeq 1000
10N.270.38	16S	Illumina HiSeq 1000
10N.270.39	16S	Illumina HiSeq 1000
10N.271.37	16S	Illumina HiSeq 1000
10N.271.38	16S	Illumina HiSeq 1000
10N.271.39	16S	Illumina HiSeq 1000
10N.272.37	16S	Illumina HiSeq 1000
10N.272.38	16S	Illumina HiSeq 1000
10N.272.39	16S	Illumina HiSeq 1000
10N.273.37	16S	Illumina HiSeq 1000
10N.273.38	16S	Illumina HiSeq 1000
10N.273.39	16S	Illumina HiSeq 1000
10N.274.37	16S	Illumina HiSeq 1000
10N.274.38	16S	Illumina HiSeq 1000
10N.274.39	16S	Illumina HiSeq 1000
10N.275.37	16S	Illumina HiSeq 1000
10N.275.38	16S	Illumina HiSeq 1000
10N.275.39	16S	Illumina HiSeq 1000
10N.276.37	16S	Illumina HiSeq 1000
10N.276.38	16S	Illumina HiSeq 1000
10N.276.39	16S	Illumina HiSeq 1000
10N.277.37	16S	Illumina HiSeq 1000
10N.277.38	16S	Illumina HiSeq 1000
10N.277.39	16S	Illumina HiSeq 1000
10N.278.37	16S	Illumina HiSeq 1000
10N.278.38	16S	Illumina HiSeq 1000
10N.278.39	16S	Illumina HiSeq 1000
10N.279.37	16S	Illumina HiSeq 1000
10N.279.38	16S	Illumina HiSeq 1000
10N.279.39	16S	Illumina HiSeq 1000
10N.280.37	16S	Illumina HiSeq 1000
10N.280.38	16S	Illumina HiSeq 1000
10N.280.39	16S	Illumina HiSeq 1000
10N.281.37	16S	Illumina HiSeq 1000
10N.281.38	16S	Illumina HiSeq 1000
10N.281.39	16S	Illumina HiSeq 1000
10N.282.37	16S	Illumina HiSeq 1000

10N.282.38	16S	Illumina HiSeq 1000
10N.282.39	16S	Illumina HiSeq 1000
10N.283.37	16S	Illumina HiSeq 1000
10N.283.38	16S	Illumina HiSeq 1000
10N.283.39	16S	Illumina HiSeq 1000
10N.284.37	16S	Illumina HiSeq 1000
10N.284.38	16S	Illumina HiSeq 1000
10N.284.39	16S	Illumina HiSeq 1000
10N.285.37	16S	Illumina HiSeq 1000
10N.285.38	16S	Illumina HiSeq 1000
10N.285.39	16S	Illumina HiSeq 1000
10N.286.37	16S	Illumina HiSeq 1000
10N.286.38	16S	Illumina HiSeq 1000
10N.286.39	16S	Illumina HiSeq 1000
10N.287.37	16S	Illumina HiSeq 1000
10N.287.38	16S	Illumina HiSeq 1000
10N.287.39	16S	Illumina HiSeq 1000
10N.288.37	16S	Illumina HiSeq 1000
10N.288.38	16S	Illumina HiSeq 1000
10N.288.39	16S	Illumina HiSeq 1000
10N.289.37	16S	Illumina HiSeq 1000
10N.289.38	16S	Illumina HiSeq 1000
10N.289.39	16S	Illumina HiSeq 1000
10N.290.37	16S	Illumina HiSeq 1000
10N.290.38	16S	Illumina HiSeq 1000
10N.290.39	16S	Illumina HiSeq 1000
10N.291.37	16S	Illumina HiSeq 1000
10N.291.38	16S	Illumina HiSeq 1000
10N.291.39	16S	Illumina HiSeq 1000
10N.292.37	16S	Illumina HiSeq 1000
10N.292.38	16S	Illumina HiSeq 1000
10N.292.39	16S	Illumina HiSeq 1000
10N.293.37	16S	Illumina HiSeq 1000
10N.293.38	16S	Illumina HiSeq 1000
10N.293.39	16S	Illumina HiSeq 1000
10N.294.37	16S	Illumina HiSeq 1000
10N.294.38	16S	Illumina HiSeq 1000
10N.294.39	16S	Illumina HiSeq 1000
10N.295.37	16S	Illumina HiSeq 1000
10N.295.38	16S	Illumina HiSeq 1000
10N.295.39	16S	Illumina HiSeq 1000
10N.296.37	16S	Illumina HiSeq 1000
10N.296.38	16S	Illumina HiSeq 1000
10N.296.39	16S	Illumina HiSeq 1000

Supplementary Table 4. Inflation values used in MCL clustering and effect on OTU inclusion in clusters.

Inflation	Fraction in	
	+/+ Clusters	+/- Clusters
1.6	100%	100%
2.0	100%	100%
2.2	100%	100%
2.4	99%	100%
2.8	100%	99%
3.2	96%	100%
3.6	85%	84%
4.0	76%	74%